Progress In Electromagnetics Research M, Vol. 8, 249–261, 2009

POLARIZED PHOTON GENERATION FOR THE TRANSPORT OF QUANTUM STATES: A CLOSED-SYSTEM SIMULATION APPROACH

M. Mijanur Rahman and P. K. Choudhury

Faculty of Engineering
Multimedia University
Cyberjaya 63100, Selangor, Malaysia

Abstract—A novel approach for logic state dependent generation of polarized photon is proposed, where the logic states '0' and '1' are represented by two sub-spaces in the Hilbert space of the hyperfine states of rubidium atom (^{87}Rb). Each subspace consists of a ground state, an intermediate state and an excited state. The atom is placed at the center of a two-mode cavity, and the cavity modes correspond to frequencies of the generated photon. Photon generation process involves raising the atom to the excited state within the corresponding subspace and letting it decay back to the initial (ground) state, emitting thereby a photon of logic state dependent polarization. In order to keep the driving laser frequencies far off from the cavity mode frequencies, the atom is raised to the excited state in two steps — first from the ground state to the intermediate state and then from the intermediate state to the excited state. Polarization states of the photon represent the logic states, and can be used to transport logic from one node to another of the quantum network.

1. INTRODUCTION

Photon has been identified as an ideal carrier for logic transport from one node to another of the envisioned quantum network. Right- and left-circular polarization states of photon can effectively represent logic states of the flying qubit. These polarization states are binary in nature and can be propagated over long distances without significant degradation.

Recently, transferring quantum state from one quantum node to another using photon as a carrier has drawn considerable attention of

Corresponding author: P. K. Choudhury (pankaj.kumar.choudhury@mmu.edu.my).

the relevant R & D community. This is evident from the research reports appearing in the literature [1–12]. Investigators have put much effort to find suitable quantum structures and processes for the generation of photons as flying qubits. At the state-of-the-art, photon is generally emitted as a result of transition from a higher energy level to a lower one of an atom or a nanodot. In the case of information transmission through optical fibers (or waveguides) or special type of fibers [13–17], photons are identified as such qubits [18].

Several approaches for the generation of photon as a flying qubit have been put forward. Gardinar [19] and Carmichael [20] proposed two-atom systems for using photon output from the first atom to drive the second atom. While the system proposed by Gardinar [19] was based on quantum Langevin equations and the fundamental equation for the two-atom system, Carmichael [20] described a quantum trajectory based theory.

A well-accepted approach for communicating spin-state of an atom to a spatially separated atom was proposed by Cirac et al. [8]. In their scheme, a quantum node consisted of an atom and a coupled cavity. They formulated Hamiltonian for describing the interaction between the atom and the corresponding cavity mode. A cavity assisted Raman process generated the photon wavepacket which, in their scheme, must be time-symmetric, in order to reproduce the spin state of the transmitting atom into the receiving one.

The time-symmetry requirement of the generated photon wavepacket in Ref. [8] was eliminated in the proposition made by Yao et al. [21]. In this proposition, photon transmission and reception processes could be independently controlled. Under the Weisskopf-Wigner approximation, the authors derived the equation of motion for resonant Raman process for a Λ-type three-level system. Their major achievement was the technique of designing a laser pulse shape for a desired shape of the output photon wavepacket.

The present work is motivated by the fact that, in spite of photon polarization state being potential representation of flying qubit logic state, attempts to generate and utilize photon polarization state for quantum state transfer between quantum nodes are hardly seen. Secondly, comprehensive simulation scheme for transmission of quantum states between quantum nodes is hardly available. As such, in the present communication, we focus on the simulation of polarized photon generation depending on the logic state of the transmitting node. However, Rahman and Choudhury [22] previously presented a simulation scheme for the cavity-assisted Raman interaction at the spin-photon interface of the transmitting node. The Raman interaction based conversion of spin qubit to photon was demonstrated

in the simulation, and the obtained results revealed that, for a designed shape of the input laser pulse, a corresponding output photon wavepacket shape could be produced. In our work, flying qubit logic states are represented by right- and left-circular polarization states of photon. This representation has the advantage that, as mentioned above, circular polarization states are binary in nature, and can be communicated to long distances without much degradation. We propose a novel approach for utilizing atomic states and processes to generate circularly polarized photon for transporting quantum state, and validate the approach through a closed-system simulation technique.

2. OVERVIEW

The transmit interface in the proposed approach consists of a multi-level atom (^{87}Rb) placed at the center of a two-mode cavity. Two subspaces $||0\rangle\rangle$ and $||1\rangle\rangle$ are identified in the Hilbert space of the atomic states. These two subspaces, as defined by Eqs. (1a) and (1b) for the

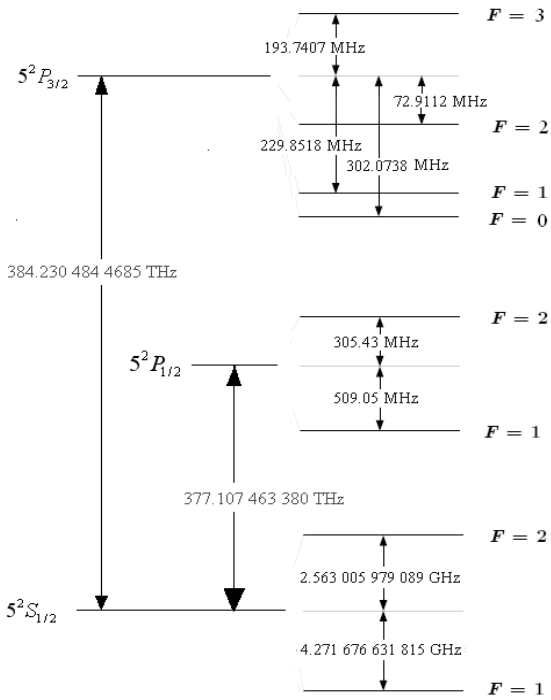

Figure 1. Selected hyperfine states of rubidium ^{87}Rb [17].

hyperfine states (Fig. 1) of ^{87}Rb atom [23], represent the logic '0' and the logic '1' states, respectively. That is, when the atom is in one of the states of the subspace $||0\rangle\rangle$, it is in the logic state '0', and when it is in one of the states of the subspace $||1\rangle\rangle$, it is in the logic state '1'.

$$||0\rangle\rangle \equiv \{(5^2S_{1/2}, F=1, m_F=1), (5^2P_{1/2}, F=1, m_F=1), (5^2P_{1/2}, F=2, m_F=2)\} \quad (1a)$$

$$||1\rangle\rangle \equiv \{(5^2S_{1/2}, F=1, m_F=-1), (5^2P_{1/2}, F=1, m_F=-1), (5^2P_{3/2}, F=2, m_F=-2)\} \quad (1b)$$

Intra-subspace transitions (Fig. 2) are initiated by the application of lasers. The laser $L0_0$ excites the atom from $|0\rangle_0 \equiv (5^2S_{1/2}, F=1, m_F=1)$ to $|0\rangle_1 \equiv (5^2P_{1/2}, F=1, m_F=1)$ and the laser $L0_1$ drives the atom from $|0\rangle_1$ to $|0\rangle_2 \equiv (5^2P_{1/2}, F=2, m_F=2)$. Similarly, $L1_0$ and $L1_1$ lasers drive the transitions from $|1\rangle_0 \equiv (5^2S_{1/2}, F=1, m_F=-1)$ to $|1\rangle_1 \equiv (5^2P_{1/2}, F=1, m_F=-1)$ and from $|1\rangle_1$ to $|1\rangle_2 \equiv (5^2P_{3/2}, F=2, m_F=-2)$, respectively. During the transitions $|0\rangle_0 \rightarrow |0\rangle_1$ and $|1\rangle_0 \rightarrow |1\rangle_1$, π-polarized photons are absorbed. During the $|0\rangle_1 \rightarrow |0\rangle_2$ and the $|1\rangle_1 \rightarrow |1\rangle_2$ transitions, respectively, photons with right-circular and left-circular polarizations are absorbed. Finally, the cavity-coupled transitions $|0\rangle_2 \rightarrow |0\rangle_0$ and $|1\rangle_2 \rightarrow |1\rangle_0$, respectively, emit photons with right-circular and left-circular polarizations into the cavity. The two modes of the cavity correspond to these last two transitions.

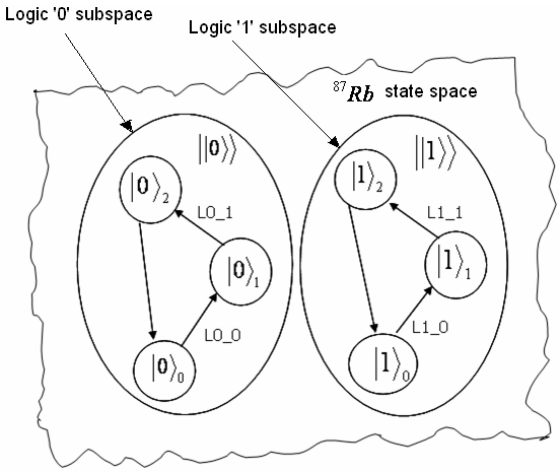

Figure 2. Subspaces of ^{87}Rb state space corresponding to the logics states '0' and '1'.

It is to be noted down that, while transferring the quantum state from one node to another, the exact cyclic transitions $|0\rangle_0 \rightarrow |0\rangle_1 \rightarrow |0\rangle_2 \rightarrow |0\rangle_0$ and $|1\rangle_0 \rightarrow |1\rangle_1 \rightarrow |1\rangle_2 \rightarrow |1\rangle_0$ are forbidden [24]. However, the transitions back to the neighborhoods of $|0\rangle_0$ and $|1\rangle_0$ are possible. Thus, the subspaces $||0\rangle\rangle$ and $||1\rangle\rangle$, respectively, consist of three neighborhoods around the states $|0\rangle_0$, $|0\rangle_1$ and $|0\rangle_2$, and $|1\rangle_0$, $|1\rangle_1$ and $|1\rangle_2$. These neighborhoods are pictorially illustrated in Fig. 3.

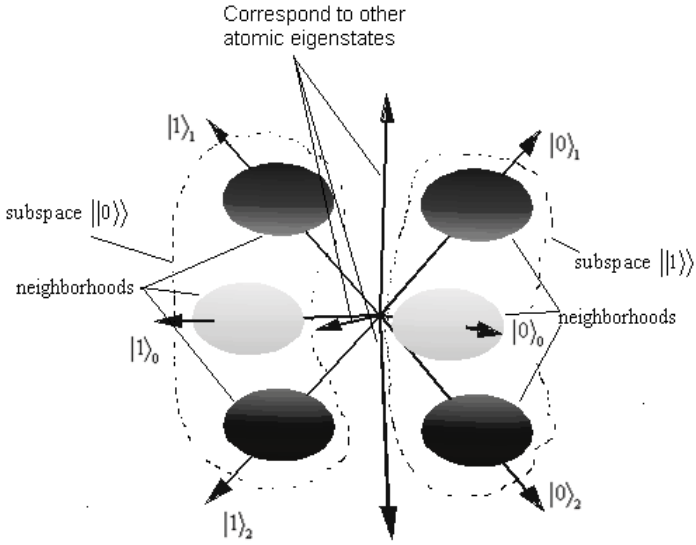

Figure 3. Neighborhoods in the subspaces $||0\rangle\rangle$ and $||1\rangle\rangle$ of the Hilbert space.

3. WORKING PRINCIPLE

The rubidium atom at the transmit interface is initially prepared to be at the ground states $|0\rangle_0$ or $|1\rangle_0$ corresponding to logic states '0' or '1', respectively. The basic idea is to raise the atom to the state $|0\rangle_2$ for the logic '0' or to the $|1\rangle_2$ state for the logic '1', and then to let it decay to the states $|0\rangle_0$ or $|1\rangle_0$ with the emission of right- or left-circularly polarized photon. The two cavity modes correspond to the transitions $|0\rangle_2 \rightarrow |0\rangle_0$ and $|1\rangle_2 \rightarrow |1\rangle_0$, and thus, accelerate the emission processes.

Two laser beams corresponding to the transitions $|0\rangle_0 \rightarrow |0\rangle_2$ and $|1\rangle_0 \rightarrow |1\rangle_2$ could be directly used to raise the atom to $|0\rangle_2$ and $|1\rangle_2$

states, respectively. However, that would introduce Rabi oscillations with multi-photon states in the cavity, which is clearly undesirable. Instead, first, lasers $L0_0$ and $L1_0$ are applied simultaneously. If the atom is in the state $|0\rangle_0$, it absorbs a photon from the laser $L0_0$, and jumps to the state $|0\rangle_1$. On the other hand, if the atom is in the state $|1\rangle_0$, it absorbs a photon from the laser $L1_0$, and jumps to the state $|1\rangle_1$. Then, lasers $L0_1$ and $L1_1$ are simultaneously applied on the atom. If the atom is in the logic state '0', it absorbs a right-circularly polarized photon from the $L0_1$ laser, and jumps to the $|0\rangle_2$ state. Similarly, for logic state '1', the atom absorbs a left-circularly polarized photon, and makes a transition to the state $|1\rangle_2$. Then, through spontaneous emission and cavity modes coupling, the atom comes back to $|0\rangle_0$ or $|1\rangle_0$ state. During the atomic decay $|0\rangle_2 \rightarrow |0\rangle_0$, a right-circularly polarized photon is emitted, and during the $|1\rangle_2 \rightarrow |1\rangle_0$ transition, a left-circularly polarized photon.

Because the laser frequencies corresponding to the transitions $|0\rangle_0 \rightarrow |0\rangle_1$, $|0\rangle_1 \rightarrow |0\rangle_2$, $|1\rangle_0 \rightarrow |1\rangle_1$ and $|1\rangle_1 \rightarrow |1\rangle_2$ are far off from the cavity mode frequencies, Rabi oscillations with multi-photon states are thus avoided.

The generated photon leaks out of the cavity, and reaches the other end through the connecting physical medium. The polarization detectors at the receiving end detect the photon polarization state implying the atomic state at the sending end.

4. SYSTEM MODEL

The Jaynes-Cumming (JC) model [25] is traditionally used to analyze two-level atom coupled to a cavity with or without a driving laser. This model provides a system Hamiltonian, which is of the following form,

$$\widehat{H}_{total} = \hat{H}_{atom} + \hat{H}_{field} + \hat{H}_{JC} = \frac{1}{2}\hbar\omega_a\hat{\sigma}_z + \hbar\omega\hat{a}^*\hat{a} - i\hbar g(\hat{a}\hat{\sigma}_+ - \hat{a}^*\hat{\sigma}_-) \quad (2)$$

where ω and ω_a are, respectively, the atomic transition frequency and the cavity mode frequency, and $\hat{a}$ and $\hat{a}^*$ are the bosonic annihilation and creation operators, respectively. Also, g is the atom-cavity mode coupling constant, and $\hat{\sigma}_+$, $\hat{\sigma}_-$ and $\hat{\sigma}_z$ are, respectively, the atomic raising, lowering and inversion operators.

However, the JC model is not adequate for the present system owing to the following reasons — (i) the present system involves two separate subspaces in the Hilbert space, (ii) each subspace contains a three-level sub-system with hyperfine atomic structure, and (iii) the system involves two pairs of lasers and lasers within each pair are simultaneously applied on the atom.

In order to accommodate the hyperfine energy levels, the atomic raising and lowering operators, $\hat{\sigma}_+$ and $\hat{\sigma}_-$, are modified into new operators, $\hat{S}^*_{\pm,0}$ and $\hat{S}_{\pm,0}$. $\hat{S}^*_+$ and $\hat{S}^*_-$ are, respectively, raising operators with increased and decreased magnetic sub-levels. Similarly, $\hat{S}_+$ and $\hat{S}_-$ are lowering operators with increased and decreased magnetic sublevels, respectively. Finally, $\hat{S}^*$ and $\hat{S}$ are raising and lowering operators, respectively, without change in magnetic sub-level. In particular, lowering operators are defined as

$$\hat{S}_+ = \sum_{m_{F,g}} C(F_g, m_{F,g}, F_e, m_{F,g}+1)\,|F_g m_{F,g}\rangle\,\langle F_e m_{F,g}+1| \quad \text{(3a)}$$

$$\hat{S}_- = \sum_{m_{F,g}} C(F_g, m_{F,g}, F_e, m_{F,g}-1)\,|F_g m_{F,g}\rangle\,\langle F_e m_{F,g}-1| \quad \text{(3b)}$$

$$\text{and} \quad \hat{S} = \sum_{m_{F,g}} C(F_g, m_{F,g}, F_e, m_{F,g})\,|F_g m_{F,g}\rangle\,\langle F_e m_{F,g}| \quad \text{(3c)}$$

In Eqs. (3a), (3b) and (3c), F_g and F_e are total atomic angular momentums at the ground and excited states, respectively, and $m_{F,g}$ is the magnetic quantum number at the ground state. The Clebsch-Gordan coefficient $C(F_g, m_{F,g}, F_e, m_{F,g}+d), d = \pm 1, 0$ is defined as [26]

$$\begin{aligned} &C(F_g, m_{F,g}, F_e, m_{F,g}+d) \\ &= \langle F_g, m_{F,g}; \Delta F = F_e - F_g, \Delta m_F = +d | F_e, m_{F,\,e} = m_{F,g} + \Delta m_F \rangle\,. \end{aligned} \quad (4)$$

where Δm_F is the change in the magnetic quantum number. The system Hamiltonian can now be written as follows:

$$\begin{aligned} \hat{H} &= \hbar\omega_a \hat{a}^*\hat{a} + \hbar\omega_b \hat{b}^*\hat{b} + \sum_i (E_i + g_{F_i} m_{F_i}\beta)\ |J_i\ F_i\ m_{F_i}\rangle\,\langle J_i\ F_i\ m_{F_i}| \\ &+\hbar\eta_{10}\left(\omega^{(0)}_{10}\hat{a}^{(0)*}_{10}\hat{a}^{(0)}_{10} + \omega^{(1)}_{10}\hat{a}^{(1)*}_{10}\hat{a}^{(1)}_{10}\right) + \hbar\eta_{21}\left(\omega^{(0)}_{21}\hat{a}^{(0)*}_{21}\hat{a}^{(0)}_{21} + \omega^{(1)}_{21}\hat{a}^{(1)*}_{21}\hat{a}^{(1)}_{21}\right) \\ &-i\hbar g(\hat{a}\hat{S}^*_+ - \hat{a}^*\hat{S}_+) - i\hbar g(\hat{b}\hat{S}^*_- - \hat{b}^*\hat{S}_-) \\ &-i\hbar\eta_{10}\, g^{(0)}_{10}(\hat{a}^{(0)}_{10}\hat{S}^{(0)*}_{10} - \hat{a}^{(0)*}_{10}\hat{S}^{(0)}_{10}) - i\hbar\eta_{10}\, g^{(1)}_{10}(\hat{a}^{(1)}_{10}\hat{S}^{(1)*}_{10} - \hat{a}^{(1)*}_{10}\hat{S}^{(1)}_{10}) \\ &-i\hbar\eta_{21}\, g^{(0)}_{21}(\hat{a}^{(0)}_{21}\hat{S}^{(0)*}_{21} - \hat{a}^{(0)*}_{21}\hat{S}^{(0)}_{21}) - i\hbar\eta_{21}\, g^{(1)}_{21}(\hat{a}^{(1)}_{21}\hat{S}^{(1)*}_{21} - \hat{a}^{(1)*}_{21}\hat{S}^{(1)}_{21}) \end{aligned} \quad (5)$$

In Eq. (5), E_i represents the energy of the atomic level $|J_i F_i m_{F_i}\rangle$, g_{F_i} is the Lande g-factor, $\beta = \mu_B B/\hbar$, μ_B is the Bohr magneton and B is the strength of the external magnetic field. Also, $\hat{a}$ and $\hat{b}$ are the annihilation operators of the two cavity modes, and $\hat{a}^{(0)}_{10}$ and $\hat{a}^{(1)}_{10}$ are, respectively, the annihilation operators corresponding to the $L0_0$ and $L1_0$ laser modes. Similarly, $\hat{a}^{(0)}_{21}$ and $\hat{a}^{(1)}_{21}$ are the annihilation operators corresponding to the $L0_1$ and $L1_1$ laser modes, respectively. Also,

$\omega_{10}^{(0)}$ and $\omega_{10}^{(1)}$ represent, respectively, frequencies of laser modes $L0_0$ and $L1_0$. $S_{10}^{(0)*}$ and $S_{10}^{(0)}$ are, respectively, the atomic raising and lowering operators in the $|0\rangle_0 \rightarrow |0\rangle_1$ transition, and $S_{10}^{(1)*}$ and $S_{10}^{(1)}$ represent raising and lowering operators, respectively, in the transition $|1\rangle_0 \rightarrow |1\rangle_1$. Similarly, $\omega_{21}^{(0)}$ and $\omega_{21}^{(1)}$ represent frequencies of laser modes $L0_1$ and $L1_1$, respectively. $S_{21\pm}^{(0)*}$ and $S_{21\pm}^{(0)}$ are, respectively, the atomic raising and lowering operators in the $|0\rangle_1 \rightarrow |0\rangle_2$ transition, and $S_{21\pm}^{(1)*}$ and $S_{21\pm}^{(1)}$ are the raising and lowering operators, respectively, in the transition $|1\rangle_1 \rightarrow |1\rangle_2$. Finally, η_{10} and η_{21} are defined as follows.

$$\eta_{10} = \begin{cases} 1 & \text{when lasers } L0_0 \text{ and } L1_0 \text{ are turned on} \\ 0 & \text{otherwise} \end{cases}$$

$$\eta_{21} = \begin{cases} 1 & \text{when lasers } L0_1 \text{ and } L1_1 \text{ are turned on} \\ 0 & \text{otherwise} \end{cases} .$$

For simplicity, the Hamitonian is generally transformed into the frame rotating at the frequency of the laser. However, as there are four different lasers in the present case with different frequencies and polarizations, the transformation is not done. Instead, in order to avoid the dealings with too big or too small numbers, all the terms in the Hamitonian are converted into the atomic unit.

5. SYSTEM EVOLUTION

We deal with the state of the system described above using the density matrix formalism, and adopt the von Neumann equation [27] for the evolution of the density matrix. The evolution equation is given as follows:

$$\frac{d}{dt}\rho(t) = \frac{1}{i\hbar}\left[\hat{H},\ \rho(t)\right] \tag{6}$$

where, $\rho(t)$ is the density matrix of the system. For simplicity of the analysis, we have not included terms describing the interaction of the system with the environment. Therefore, Eq. (6) essentially describes a closed system evolution.

6. SIMULATION AND RESULTS

In order to perform a closed system investigation, we developed a simulation program. While Eq. (6) provides equation of motion for the simulation, Eq. (5) provides the Hamiltonian. Our simulation approach includes a control module to provide the timing update trigger after

every small time interval Δt, and an execution module to update $\rho(t)$ after every interval of Δt. The rate of change of $\rho(t)$ is calculated according to Eq. (6), and $\rho(t)$ is updated using the following numerical approximation:

$$\rho(t_0 + \Delta t) = \rho(t_0) + \frac{d}{dt}\rho(t)\bigg|_{t_0} \Delta t \tag{7}$$

The Hilbert space for the system is obtained by taking the tensor product of the Hilbert spaces for atom, cavity modes and laser modes as follows:

$$H = H_{atom} \otimes H_{cav0} \otimes H_{cav1} \otimes H_{L0_0} \otimes H_{L1_0} \otimes H_{L0_1} \otimes H_{L1_1} \tag{8}$$

where H is the combined Hilbert space, H_{atom} is the atomic Hilbert space, and H_{cav0} and H_{cav1} are, respectively, the Hilbert spaces (Fock spaces) for cavity modes. Also, H_{L0_0}, H_{L1_0}, H_{L0_1} and H_{L1_1} are the Hilbert spaces (Fock spaces) for the laser modes.

For simplicity of computation, we have considered two laser modes $L0_1$ and $L1_1$ in the simulation. It is assumed that at the start of the simulation, the atom is pre-excited by the other two laser modes ($L0_0$ and $L1_0$) to state $|0\rangle_1$ or $|1\rangle_1$ depending on the logic state.

Simulation results with the initial state $|0\rangle_1$ (that is, the logic state '0') are shown in Figs. 4, 5 and 6. In these figures, the horizontal axes represent time in the atomic unit (a.u.) and the vertical axes show the probability of occupation of the three states within the subspace $||0\rangle\rangle$. Figs. 4 and 5 show that, as the laser modes $L0_1$ and $L1_1$ are applied, the ^{87}Rb atom makes a rapid transition from the state $|0\rangle_1$ to the $|0\rangle_2$ state. Figs. 5 and 6 together show that afterwards the atom makes relatively slow transition from the $|0\rangle_2$ state to the state $|0\rangle_0$. Because the system under consideration is essentially a closed one, the right-circularly polarized photon, emitted during the transition $|0\rangle_2 \rightarrow |0\rangle_0$, remains in the cavity and causes the $|0\rangle_0 \rightarrow |0\rangle_2$ transition. Figs. 5 and 6 clearly illustrate the resulting oscillations between the states $|0\rangle_2$ and $|0\rangle_0$.

Similar results were obtained when started with the initial state $|1\rangle_1$ (i.e., the logic state '1'). The results are shown in Figs. 7, 8 and 9. It is clear from Figs. 7 and 8 that the application of laser modes $L0_1$ and $L1_1$ has caused the atom to make transition $|1\rangle_1 \rightarrow |1\rangle_2$. From Figs. 8 and 9, we notice that, afterwards, the atom makes relatively slow transition from the state $|1\rangle_2$ to the state $|1\rangle_0$. As the system is isolated from the environment, the emitted left circularly polarized photon remains in the cavity and causes the $|1\rangle_0 \rightarrow |1\rangle_2$ transitions. The resulting oscillations between states $|1\rangle_0$ and $|1\rangle_2$ are seen in Figs. 8 and 9.

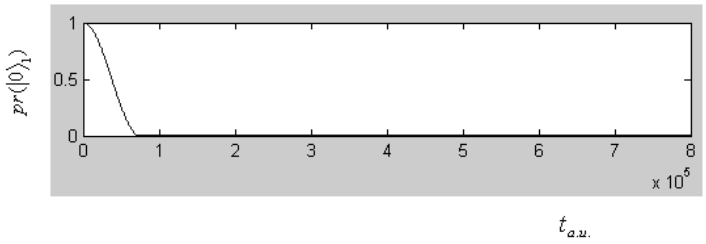

Figure 4. Probability of occupation of the state $|0\rangle_1$.

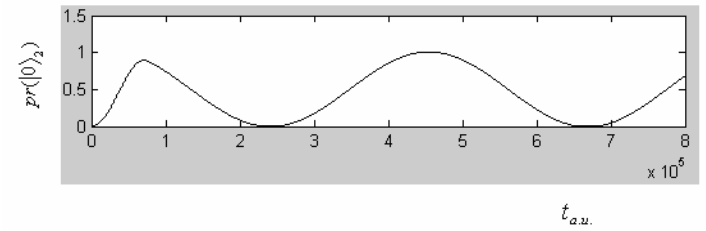

Figure 5. Probability of occupation of the state $|0\rangle_2$.

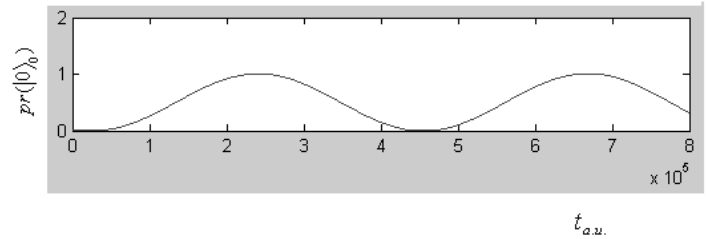

Figure 6. Probability of occupation of the state $|0\rangle_0$.

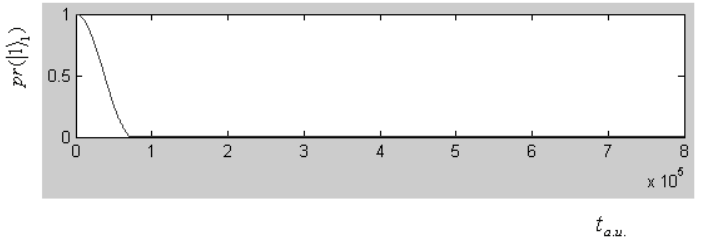

Figure 7. Probability of occupation of the state $|1\rangle_1$.

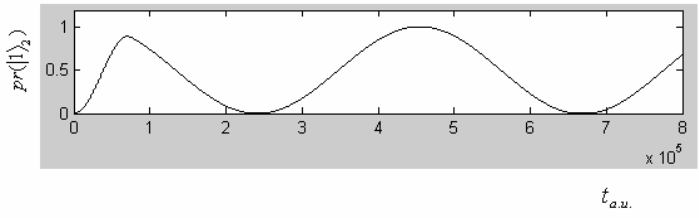

Figure 8. Probability of occupation of the state $|1\rangle_2$.

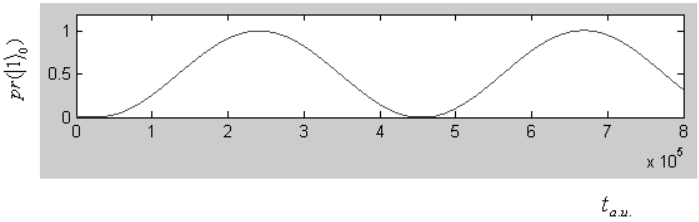

Figure 9. Probability of occupation of the state $|1\rangle_0$.

7. CONCLUSION

From the foregoing discussions, it may be inferred that a novel approach is proposed for generation of polarized photons for transport of quantum state from one node to another in a quantum network. The logic states have been represented by the two subspaces within the Hilbert space in such a way that during photon absorption and emission for quantum state transfer, the atom remains in the same subspace. A simulation platform has been presented for the evolution of the density matrix. A system Hamiltonian has been formulated for the purpose. The simulation results show the efficacy of the approach, where the probability of occupation of the ground and the excited states are determined, and it is expected that the obtained results will be found much applicable in further investigation of the photon wavepacket transmission in quantum networks.

REFERENCES

1. Monroe, C., D. N. Meekhof, B. E. King, W. M. Itano, and D. J. Wineland, "Demonstration of a fundamental quantum logic gate," *Phys. Rev. Lett.*, Vol. 75, 4714–4717, 1995.

2. Loss, D. and D. P. DiVincenzo, "Quantum computation with quantum dots," *Phys. Rev. A*, Vol. 57, 120–126, 1998.
3. Fan, X. D., P. Palinginis, S. Lacey, H. L. Wang, and M. C. Longeran, "Coupling semiconductor nanocrystals to a fused-silica microsphere — A quantum-dot microcavity with extremely high Q factors," *Opt. Lett.*, Vol. 25, 1600–1602, 2000.
4. Chen, P., C. Piermarocchi, L. J. Sham, D. Gammon, and D. G. Steel, "Theory of quantum optical control of a single spin in a quantum dot," *Phys. Rev. B*, Vol. 69, 075320–075327, 2004.
5. Blinov, B. B., D. L. Moehring, L.-M. Duan, and C. Monroe, "Observation of entanglement between a single trapped atom and a single photon," *Nature*, Vol. 428, 153–157, 2004.
6. Mijanur Rahman, M. and P. K. Choudhury, "A review of the state-of-the-art of particle physics with extra dimensions," *Asian J. Phys.*, Vol. 17, 263–272, 2008.
7. Cirac, J. I. and P. Zoller, "Quantum computations with cold trapped ions," *Phys. Rev. Lett.*, Vol. 74, 4091–4094, 1995.
8. Cirac, J. I., P. Zoller, H. J. Kimble, and H. Mabuchi, "Quantum state transfer and entanglement distribution among distant nodes in a quantum network," *Phys. Rev. Lett.*, Vol. 78, 3221–3224, 1997.
9. Cirac, J. I., A. K. Ekert, S. F. Huelga, and C. Macchiavello, "Distributed quantum computation over noisy channels," *Phys. Rev. A*, Vol. 59, 4249–4254, 1999.
10. Scherer, A., O. Painter, J. Vuckovic, M. Loncar, and T. Yoshie, "Photonic crystals for confining, guiding, and emitting light," *IEEE Trans. on Nanotech.*, Vol. 1, 4–11, 2002.
11. De Sousa, R. and S. Das Sarma, "Theory of nuclear-induced spectral diffusion: Spin decoherence of phosphorus donors in Si and GaAs quantum dots," *Phys. Rev. B*, Vol. 68, 115322–115334, 2003.
12. Yao, W., R. B. Lin, and L. J. Sham, "Nanodot-cavity electrodynamics and photon entanglement," *Phys. Rev. Lett.*, Vol. 92, 217402–217405, 2004.
13. Villa-Villa, F., J. A. Gaspar-Armenta, and A. Mendoza-Suárez, "Surface modes in one dimensional photonic crystals that include left handed materials," *Journal of Electromagnetic Waves and Applications*, Vol. 21, No. 4, 485–499, 2007.
14. Wang, Z.-Y., X.-M. Cheng, X.-Q. He, S.-L. Fan, and W. Z. Yan, "Photonic crystal narrow filters with negative refractive index structural defects," *Progress In Electromagnetics Research*, PIER 80, 421–430, 2008.

15. Abd-Rahman, F., P. K. Choudhury, D. Kumar, and Z. Yusoff, "An analytical investigation of four-layer dielectric optical fibers with au nano-coating — A comparison with three-layer optical fibers," *Progress In Electromagnetics Research*, PIER 90, 269–286, 2009.
16. Qi, L.-M. and Z. Yang, "Modified plane wave method analysis of dielectric plasma photonic crystal," *Progress In Electromagnetics Research*, PIER 91, 319–332, 2009.
17. Watanabe, K. and K. Yasumoto, "Accuracy improvement of the Fourier series expansion method for floquet-mode analysis of photonic crystal waveguides," *Progress In Electromagnetics Research*, PIER 92, 209–222, 2009.
18. Lee, H.-S., "A photon modeling method for the characterization of indoor optical wireless communication," *Progress In Electromagnetics Research*, PIER 92, 121–136, 2009.
19. Gardiner, C. W., "Driving a quantum system with the output field from another driven quantum system," *Phys. Rev. Lett.*, Vol. 70, 2269–2272, 1993.
20. Carmichael, H. J., "Quantum trajectory theory for cascaded open systems," *Phys. Rev. Lett.*, Vol. 70, 2273–2276, 1993.
21. Yao, W., R. B. Lin, and L. J. Sham, "Theory of control of the spin-photon interface for quantum networks," *Phys. Rev. Lett.*, Vol. 95, 030504–030507, 2005.
22. Mijanur Rahman, M. and P. K. Choudhury, "Nanophotonic waveguidance in quantum networks — A simulation approach for quantum state transfer," *Optik*, in press.
23. Steck, D. A., "Rubidium-87 D line data," available online at http://steck.us/alkalidata (revision 2.1.1, April 30, 2009).
24. Wootters, W. K. and W. H. Zurek, "A single quantum cannot be cloned," *Nature*, Vol. 299, 802–803, 1982.
25. Jaynes, E. T. and F. W. Cummings, "Comparison of quantum and semiclassical radiation theories with application to the beam maser," *Proc. IEEE*, Vol. 51, 89–109, 1963.
26. Whalen, S. J. and H. J. Carmichael, "Photon correlation functions and photon blockade in two-mode cavity QED," *Symposium of the Dodd-walls Centre for Quantum Science and Technology*, Paper TuP26, Queenstown (New Zealand), December 9–11, 2008.
27. Wang, S. J., D. Zhao, H. G. Luo, L. X. Cen, and C. L. Jia, "Exact solution to the von Neumann equation of the quantum characteristic function of the two-level Jaynes-Cummings model," *Phys. Rev. A*, Vol. 64, 052102–052105, 2001.